

5-3-2019

Thermodynamic Studies of the Binding of RPC2, ([Ru(Ph₂phen)₃]²⁺), to Purified Tubulin and Microtubules

Savannah J. West

Follow this and additional works at: <https://scholarsjunction.msstate.edu/td>

Recommended Citation

West, Savannah J., "Thermodynamic Studies of the Binding of RPC2, ([Ru(Ph₂phen)₃]²⁺), to Purified Tubulin and Microtubules" (2019). *Theses and Dissertations*. 4711.
<https://scholarsjunction.msstate.edu/td/4711>

This Graduate Thesis - Open Access is brought to you for free and open access by the Theses and Dissertations at Scholars Junction. It has been accepted for inclusion in Theses and Dissertations by an authorized administrator of Scholars Junction. For more information, please contact scholcomm@msstate.libanswers.com.

Thermodynamic studies of the binding of RPC2, ($[\text{Ru}(\text{Ph}_2\text{phen})_3]^{2+}$), to purified tubulin and
microtubules

By

Savannah J. West

A Theses
Submitted to the Faculty of
Mississippi State University
in Partial Fulfillment of the Requirements
for the Degree of Chemistry
in Biophysical Chemistry
in the College of Arts and Sciences

Mississippi State, Mississippi

May 2019

Copyright by
Savannah J. West
2019

Thermodynamic studies of the binding of RPC2, ($[\text{Ru}(\text{Ph}_2\text{phen})_3]^{2+}$), to purified tubulin and
microtubules

By

Savannah J. West

Approved:

Edwin A. Lewis
(Major Professor)

Joseph P. Emerson
(Graduate Coordinator, Committee Member)

Nicholas C. Fitzkee
(Committee Member)

Rick Travis
Dean
College of Arts & Sciences

Name: Savannah J. West

Date of Degree: May 3, 2019

Institution: Mississippi State University

Major Field: Chemistry

Major Professor: Edwin A. Lewis

Title of Study: Thermodynamic studies of the binding of RPC2, ($[\text{Ru}(\text{Ph}_2\text{phen})_3]^{2+}$), to purified tubulin and microtubules

Pages in Study: 38

Candidate for Degree of Chemistry

Tubulin and elastin-like polypeptides (ELPs) both form large protein structures which can be thermodynamically evaluated using isothermal titration calorimetry and differential scanning calorimetry. ELPs are thermos-responsive biopolymers that undergo phase separation and form coacervates when heated. This project assesses the liquid-liquid phase separation of an ELP sequence derived from tropoelastin with a SynB1 cell-penetrating peptide attached to the N-terminus in conjunction with the chemotherapeutic drug doxorubicin. Microtubules (MTs) are a dynamic cellular structure formed of tubulin α/β -heterodimers and are responsible for several important cellular processes, making them a viable target for anti-cancer drugs. There has been extensive research done to identify new ligands that show selective binding to microtubules. Ruthenium (II) polypyridyl complexes (RPCs) have been found to promote the polymerization of tubulin into microtubules. ITC has been used to determine the binding affinity of $[\text{Ru}(\text{II})(\text{Ph}_2\text{phen})_3]^{2+}$ (RPC2).

TABLE OF CONTENTS

LIST OF TABLES	iv
LIST OF FIGURES	v
I. INTRODUCTION TO TUBULIN AND ELASTIN-LIKE POLYPEPTIDES.....	1
REFERENCES.....	5
II. REVIEW OF TECHNIQUES AND INSTRUMENTS USED IN THIS STUDY	7
REFERENCES.....	11
III. PURIFICATION OF TUBULIN USING HIGH-MOLARITY BUFFERS.....	12
REFERENCES.....	19
IV. EFFECT OF BINDING AGENTS AND DMSO ON THE POLYMERIZATION OF TUBULIN.....	20
REFERENCES.....	24
V. BIOPHYSICAL BINDING PROPERTIES OF $[RU(PH_2PHEN)_3]^{2+}$ TO MICROTUBULES	25
REFERENCES.....	33
VI. THERMAL STABILITY OF SYN-B1 ELASTIN-LIKE POLYPEPTIDE AND DOXORUBICIN.....	34
REFERENCES.....	38

LIST OF TABLES

Table 5.1	ITC-derived thermodynamic parameters for the binding of docetaxel, colchicine, and RPC2 in non-competitive and competitive experiments.....	28
Table 6.1	Thermodynamic parameters of obtained from unlabeled and Dox-labeled SynB1-Cys-ELP samples	35

LIST OF FIGURES

Figure 1.1	Microtubule stabilizing agents A. paclitaxel and B. docetaxel, which both bind to the taxane site on microtubules.	3
Figure 1.2	Ruthenium-based anticancer drugs A. KP1019 and B. NAMI-A.	4
Figure 1.3	Ruthenium-based polypyridyl complex $[\text{Ru}(\text{Ph}_2\text{phen})_3]^{2+}$	4
Figure 2.1	Polymerization assay of 2 mg/mL tubulin purchased from Cytoskeleton, Inc. Temperature was set at 37°C. The buffer was composed of 80 mM PIPES, 1 mM GTP, 1 mM MgSO_4 , 1 mM EGTA, pH 6.9.	8
Figure 2.2	Schematic of isothermal titration calorimeter. Includes example thermogram and fitted curve of the reaction enthalpy.	9
Figure 2.3	Schematic of a differential scanning calorimeter, including the reference cell (containing the solvent) and the sample cell.	10
Figure 2.4	DSC curve of a 100 μM unlabeled ELP sample, scanned at a rate of 1 °C/min in PBS buffer.	10
Figure 3.1	SDS-PAGE of lab purified protein using the Popov protocol. Gel stained with Coomassie blue. (A) Week 1 and (B) Week 2 of lab purified tubulin using the modified Popov protocol.....	16
Figure 3.2	Turbidity assay of tubulin purified using the Popov method. The tubulin was selected from tubulin purified without the addition of GDP in the cold centrifugations.	16
Figure 3.3	Turbidity assay of tubulin purchased from Cytoskeleton, Inc. and purified using the Shelanski method. Tubulin concentration is 2 mg/mL.	17
Figure 3.4	SDS Gel electrophoresis of tubulin purification using GDP. (Left to right) 1. GoldBio Bluestain protein ladder. 2. First centrifugation supernatant. 3. Second centrifugation supernatant. 4. Second centrifugation depolymerized pellet solution. 5. Third centrifugation supernatant. 6. Fourth centrifugation supernatant. (No band visible.) 7. Fifth centrifugation supernatant (final protein solution).....	17

Figure 3.5	Turbidity assay of tubulin purified using improved Popov method with GDP in the cold water baths and centrifugation steps. The tubulin selected from tubulin purified without the addition of GDP in the cold centrifugations. Note that the lack of lag period can be attributed to the temperature of the tubulin being above ice water temperature.	18
Figure 4.1	Polymerization assays of 2 mg/mL tubulin at 37°C. All concentrations were 2 mg/mL and ligand concentrations were 10 μM.	21
Figure 4.2	Polymerization assays of 2 mg/mL tubulin with 10 μM at 37°C. Tubulin was purchased from Cytoskeleton, Inc. and purified using the Shelanski method.	22
Figure 4.3	Polymerization assay of 2 mg/mL tubulin with and without 5% DMSO. The tubulin sample was purchased from Cytoskeleton, Inc. and purified using the Shelanski method. [7].....	23
Figure 5.1	Transmission electron micrographs (provided by Dr. Frederick Macdonnell) of (A) tubulin polymerized in the absence of any ligands, (B) tubulin polymerized with 10 μM paclitaxel, (C) tubulin polymerized with 10 μM RPC2. The samples were stained with 1% (w/v) uranyl acetate on 300-mesh carbon-coated, formvar-treated copper grids. The grids were studied in a Zeiss model 10CA electron microscope and the bar scale is 100 nm.	26
Figure 5.2	Nonlinear regression fits of the ITC integrated heat data for docetaxel binding to depolymerized tubulin and microtubules.	29
Figure 5.3	Nonlinear regression fit of the ITC integrated heat data for RPC2 and colchicine binding to microtubules.	29
Figure 5.4	Nonlinear regression fits of the ITC integrated heat data for competitive experiments.....	30
Figure 5.5	Thermodynamic profiles for ligand binding to polymerized and depolymerized tubulin.	32
Figure 6.1	DSC curve of unlabeled SynB1-ELP, 45% Dox-labeled SynB1-ELP, and 90% Dox-labeled SynB1-ELP scanned at a rate of 1°C/min.	36
Figure 6.2	DSC curve of unlabeled SynB1-ELP scanned at a rate of 1°C/min and 0.2°C/min.	36

CHAPTER I

INTRODUCTION TO TUBULIN AND ELASTIN-LIKE POLYPEPTIDES

Tubulin and elastin-like polypeptides (ELPs) form large protein structures which can be thermodynamically evaluated using ITC and N-DSC. ELPs are thermo-responsive biopolymers with the capability to undergo phase separation and form large coacervates when heated. Their ability to phase separate from a solvated liquid to an insoluble coacervate is a promising drug delivery vehicle that is currently under intense investigation. [1-3] A peptide sequence derived from tropoelastin is used in this study and has a SynB1 cell-penetrating peptide, SynB1-Cys-ELP1, attached to the N-terminus to improve ELP uptake through endocytosis. [4, 5]

The ELP phase separation process is concentration dependent [6] and noted by a lower critical solution temperature (LCST), above which the ELPs are not soluble and form coacervate droplets. The coacervate is formed from droplets when the interfacial tension is high enough. [7] Turbidity measurements can be used to determine the LCST, but since this does not provide quantitative information about the size of the coacervate. Dynamic light scattering is used to measure the particle size. [5] Doxorubicin, a chemotherapeutic drug used as an antitumor agent in solid tumors, was used to determine the impact of labeling on the liquid-liquid phase separation. [5, 6, 8, 9] This study uses nano-differential scanning calorimetry to determine the LCST of SynB1 ELPs. The use of SynB1-Cys-ELP1 in conjunction with doxorubicin have shown an increase in the targeting and efficacy of systemically delivered therapeutics relative to free therapeutics. [4]

Tubulin is a family of proteins whose main function is to assemble into protofilament strands, which twist and coalesce to form microtubules. Microtubules from mammalian brain tissue are primarily composed of repeating α and β heterodimers. Microtubules have a large tube-like structure with a plus and minus end where the tubulin polymerizes and depolymerizes, respectively. [10-14] Microtubules are a major component of the cytoskeleton. Motor proteins such as kinesin use the directionality of microtubules to transport vesicles and organelles throughout the cell. Microtubules are responsible for maintaining rigid cell structures and for the formation of the mitotic spindle during cell mitosis, during which they significantly increase in number and length to separate the duplicated chromosomes. [10, 11]

Cancerous cells replicate excessively, leading to an increase in the amount of microtubules formed in preparation for cell separation. This makes microtubules a viable target for anti-cancer alkylating agents. Ligands bind to microtubules and can be usually classified into two groups: stabilizers and destabilizers. Stabilizing agents bind to microtubules and prevent them from depolymerizing at the minus end and can engender significant structural changes to the microtubule. Destabilizing agents bind to microtubules and cause them to depolymerize into α/β heterodimers. These binding agents will prevent cell replication and can induce severe distortions in the integrity of the cytoskeleton. [15] Drugs currently used in anticancer therapy that target microtubules include paclitaxel and docetaxel, commercially sold as Taxol and Taxotere. (Figure 1.1) Paclitaxel is a compound found in the bark of the pacific yew tree; docetaxel is an analog of paclitaxel, produced synthetically. [16, 17] Platinum-based anticancer therapy drugs have been in use for over 40 years and is used in approximately 40% of cancer treatments. [18] However, repeated use of platinum-based drugs such as cisplatin has made some forms of cancer more resistant to treatment using these ligands. Patients often cannot be given

higher doses of platinum-based drugs because of their severe side-effects and high toxicity. This has led to an interest in ruthenium-based complexes, which have been shown to be less toxic. Two ruthenium-based anticancer drugs have proceeded to Phase I clinical trials at this time: KP1019 and NAMI-A. (Figure 1.2) [19,20] Dr. Frederick MacDonnell at the University of Texas Arlington designed and synthesized ruthenium(II) polypyridyl complexes (RPCs) used in the polymerization and isothermal titration calorimetry experiments. His research group injected their synthesized RPCs into cancerous cells which were observed and lysed. It was found that out of the RPCs used in the study, $[\text{Ru}(\text{Ph}_2\text{phen})_3]^{2+}$ (Figure 1.3) showed a high degree of preferential binding to the cytoskeleton of the cells over the nucleus, cytoplasm, or membrane-bound organelles.

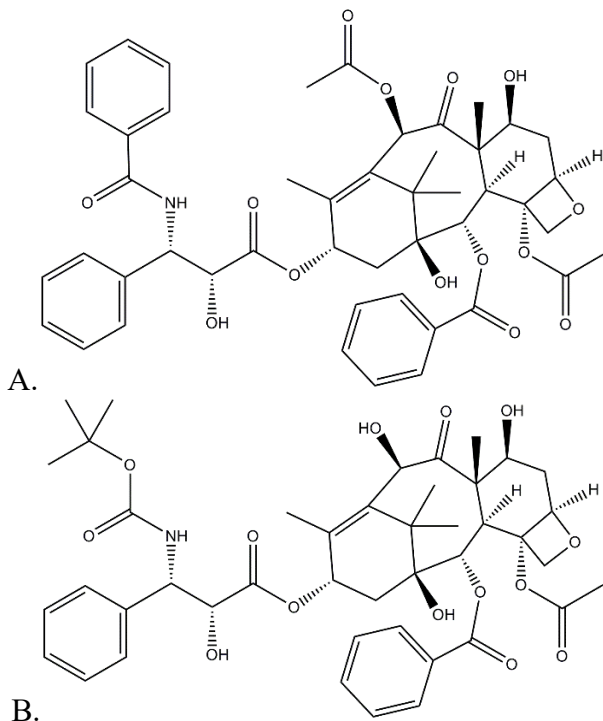


Figure 1.1 Microtubule stabilizing agents A. paclitaxel and B. docetaxel, which both bind to the taxane site on microtubules.

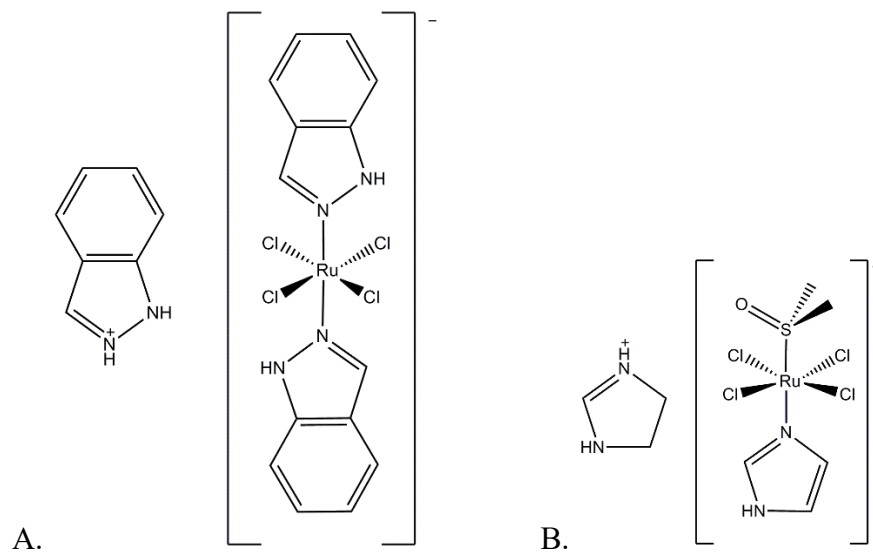


Figure 1.2 Ruthenium-based anticancer drugs A. KP1019 and B. NAMI-A.

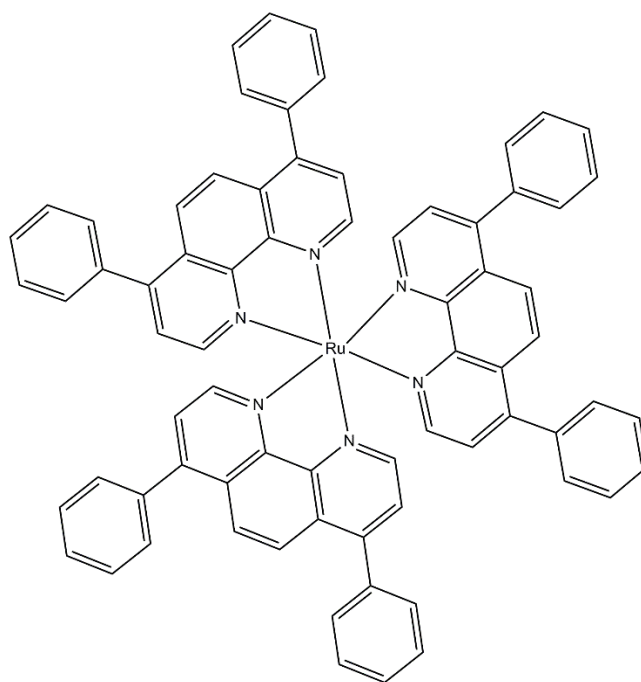


Figure 1.3 Ruthenium-based polypyridyl complex $[Ru(Ph_2phen)_3]^{2+}$.

REFERENCES

1. Cobb, J. S.; Zai-Rose, V.; Correia, J. J.; Janorkar, A. V. "Visualization of the temperature dependent rearrangement of SynB1 elastin-like polypeptide on silica using scanning electron microscopy." *Anal. Biochem.* 2018, **558**, 41-49.
2. Janorkar, A. V.; Rajagopalan, P.; Yarmush, M. L.; Megeed, Z. "The use of elastin-like polypeptide-polyelectrolyte complexes to control hepatocyte morphology and function *in vitro*." *Biomaterials*, 2008, **29**, 625-632.
3. Chilkoti, A.; Nath, N. "Creating 'Smart' Surfaces Using Stimuli Responsive Polymers." *Adv. Materials*. 2002, **14** (14), 1243-1247.
4. Lyons, D. F.; Le, V.; Bidwell, G. L.; Kramer, W. H.; Lewis, E. A.; Raucher, D.; Correia, J. J. "Structural and Hydrodynamic Analysis of a Novel Drug Delivery Vector: ELP[V₅G₃A₂-150]." *Biophys. J.* 2013, **104**, 2009-2021.
5. Lyons, D. F.; Le, V.; Kramer, W. H.; Bidwell, G. L.; Lewis, E. A.; Raucher, D.; Correia, J. J. "Effect of basic cell-penetrating peptides on the structural, thermodynamic, and hydrodynamic properties of a novel drug delivery vector, ELP[V₅G₃A₂-150]." *Biochem.*, 2014, **53** (6), 1081-1091.
6. Meyer, D. E.; Chilkoti, A. "Quantification of the Effects of Chain Length and Concentration on the Thermal Behavior of Elastin-like Polypeptides." *Biomacromolecules*, 2004, **5**, 846-851.
7. Hyman, A. A.; Christoph, A. W.; Jülicher, F. "Liquid-Liquid Phase Separation in Biology." *Annu. Rev. Cell Dev. Biol.* 2014, **30**, 39-58.
8. Bidwell, G. L.; Fokt, I.; Priebe, W.; Raucher, D. "Development of elastin-like polypeptide for thermally targeted delivery of doxorubicin." *Biochem. Pharmacol.* 2007, **73**, 620-631.
9. Dreher, M. R.; Raucher, D.; Chilkoti, A. "Evaluation of an elastin-like polypeptide-doxorubicin conjugate for cancer therapy." *J. Control. Release.* 2003, **91**, 31-43.
10. Correia, J. J.; Wilson, L. (ed.) "Microtubules, *in vitro*" Academic Press: Amsterdam. 2nd Ed. 2013.
11. Wade, R. W. "On and Around Microtubules: An Overview." *Mol. Biotechnol.* 2009, **43**, 177-191.

12. Howard, J.; Hyman, A. A. "Dynamics and mechanics of the microtubule plus end." *Nature*, 2003, **422**, 753-758.
13. Mandelkow, E. M.; Mandelkow, E.; Milligan, R. A. "Microtubule Dynamics and Microtubule Caps: A Time-resolved Cryo-Electron Microscopy Study." *J. Cell Biol.* 1991, **114** (5), 977-991.
14. Roll-Mecak, A. "Microtubule severing enzymes." *Curr. Opin. Cell Biol.* 2010, **22** (1), 96-104.
15. Correia, J. J. "Effects of Antimitotic Agents on Tubulin-Nucleotide Interactions." *Pharmac. Ther.* 1991, **25**, 127-147.
16. Harrison, H. R.; Holden, K. D.; Liu, G. "Beyond Taxanes: A Review of Novel Agents That Target Mitotic Tubulin and Microtubules, Kinases, and Kinesins." *Clin. Adv. Hematol. Oncol.* 2009, **7** (1), 54-65.
17. Jordan, A.; Hadfield, J. A.; Lawrence, N. J.; McGown, A. T. "Tubulin as a Target for Anticancer Drugs: Agents Which Interact with the Mitotic Spindle." 1997. CCC 0198-6325/98/040259-38.
18. Moucheron, C. "From cisplatin to photoreactive Ru complexes: targeting DNA for biomedical applications." *New J. Chem.* 2009, **33**, 235-245.
19. Mari, C.; Pierroz, V.; Ferrari, S.; Gasser, G. "Combination of Ru(II) complexes and light: new frontiers in cancer therapy." *Chem. Sci.* 2015, **6**, 2660-2686.
20. Mikek, C. G.; Macha, V. R.; White, J. C.; Martin L. R.; West, S. J.; Butrin, A.; Shumaker, C.; Gwin, J. C.; Alatrash, N.; MacDonnell F. M.; Lewis, E. A. "The Thermodynamic Effects of Ligand Structure on the Molecular Recognition of Mono- and Biruthenium Polypyridyl Complexes with G-Quadruplex DNA." *Eur. J. Inorg. Chem.* 2017, 2953-3960.

CHAPTER II

REVIEW OF TECHNIQUES AND INSTRUMENTS USED IN THIS STUDY

The two studies in this thesis use three principal techniques to determine the effect of altering the solvent used in polymerization of tubulin, the addition of microtubule stabilizing and destabilizing ligands to tubulin, and the addition of Doxorubicin to SynB1-Cys elastin-like polypeptides.

UV-vis spectroscopy was used to determine the concentration of tubulin and to monitor the polymerization of tubulin. A Thermo Scientific NanoDrop 2000c Spectrophotometer was used for both measurements. The nanodrop spectrophotometer was used to determine protein concentration and the polymerization assays were measured in a 1 cm pathlength cuvette. Tubulin protein concentration was determined using an extinction coefficient of $\epsilon_{280} = 115,000 \text{ M}^{-1} \text{ cm}^{-1}$. [1] A typical tubulin polymerization assay was performed at a concentration of 2 mg/mL. The cuvette holder was preheated to 37°C and the cuvette and tubulin solution were kept on ice before the assay to ensure that no polymerization occurred before the initial measurement. Typical buffer conditions were: 80 mM PIPES, 1 mM GTP, 1 mM MgSO₄, 1 mM EGTA, pH 6.9. [1, 2, 3] Absorbance was recorded at 340 nm and recorded every 30 seconds for a minimum of one hour, or until the absorbance had stopped increasing or had reached a point where the measurement was no longer accurate. An example of a tubulin polymerization assay performed in this study is shown in Figure 2.1.

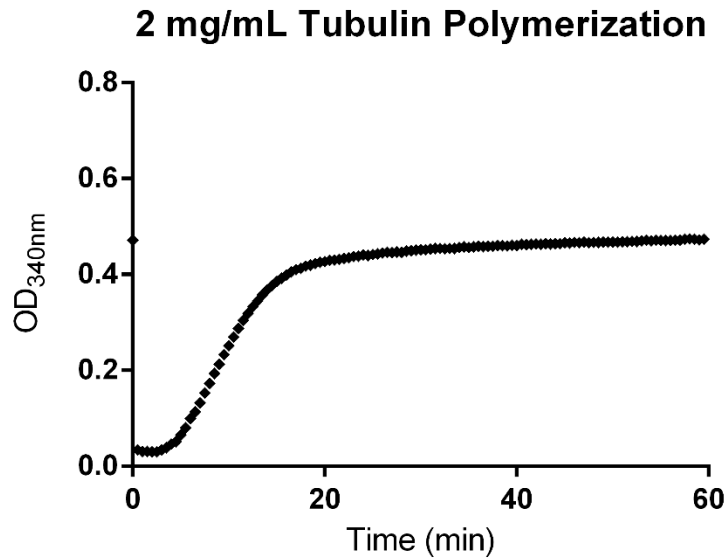


Figure 2.1 Polymerization assay of 2 mg/mL tubulin purchased from Cytoskeleton, Inc. Temperature was set at 37°C. The buffer was composed of 80 mM PIPES, 1 mM GTP, 1 mM MgSO₄, 1 mM EGTA, pH 6.9.

Isothermal titration calorimetry (ITC) was used to determine the thermodynamic binding properties of docetaxel, colchicine, and RPC2 to tubulin and microtubules. [4, 5, 6, 7] A schematic of an ITC is shown in Figure 2.2. [8] Constant heat is applied to the reference cell heater before ligand binding, directing a feedback circuit and activating a heater on the sample cell. Ligand is titrated into the sample cell and heat is either produced or absorbed. The power needed to maintain equal temperatures between the reference and sample cell is measured. The increase in the temperature of the sample cell upon addition of the ligand indicates an exothermic reaction, whereas an endothermic reaction requires an increase in the power supplied to the sample cell that is proportional to the change in temperature. A well designed ITC experiment can be used to describe the binding constant (K) between molecules. It can be applied to biomacromolecules like DNA and proteins and their interactions with ligands. The free energy term (ΔG) can be calculated by $\Delta G = -RT\ln(K)$. The integrated heat of each injection provides a

ΔH for the process, where the ΔG and ΔH used together can yield ΔS information through $\Delta G = -\Delta H - T\Delta S$.

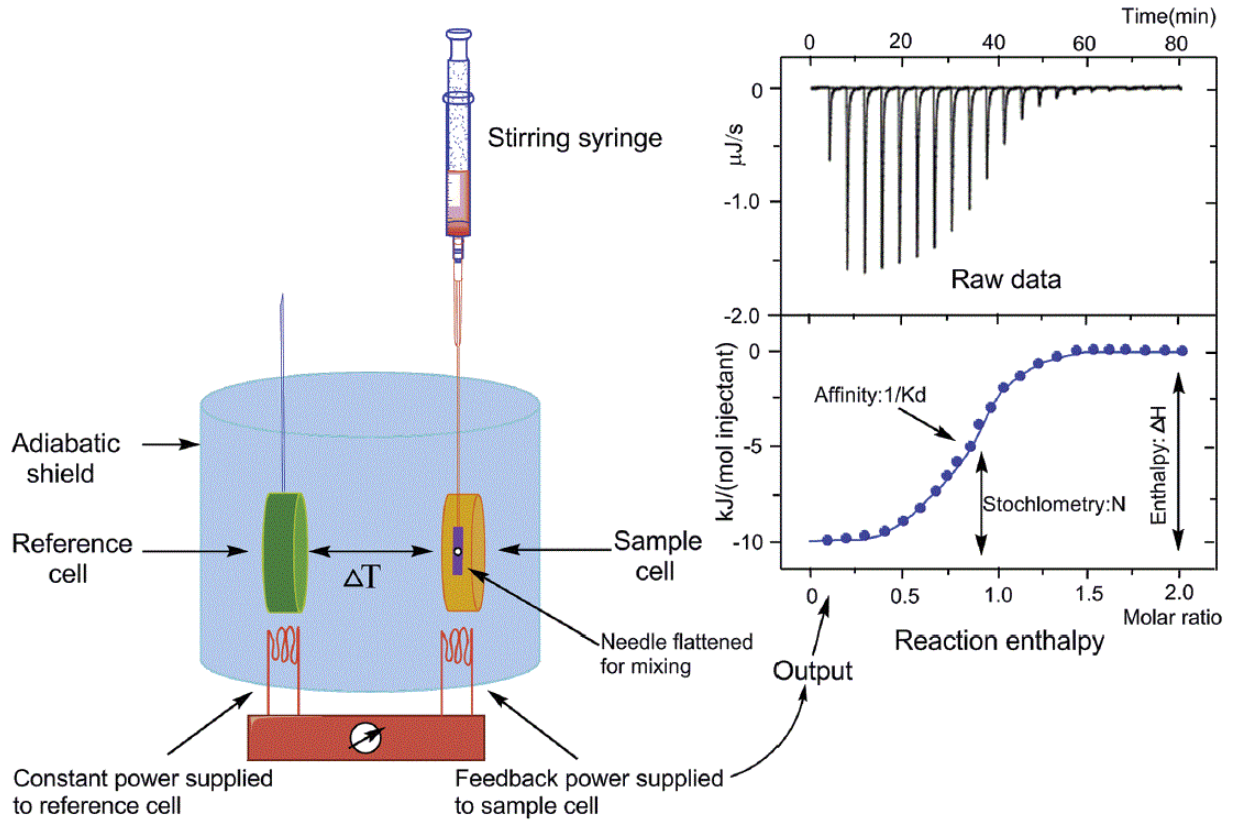


Figure 2.2 Schematic of isothermal titration calorimeter. Includes example thermogram and fitted curve of the reaction enthalpy.

Differential scanning calorimetry (DSC) was used to measure the temperature at which SynB1-Cys elastin-like polypeptides (ELP) would phase separate into a coacervate when Doxorubicin was added to the sequence. Figure 2.3 shows a schematic of the components of a DSC. A DSC measures the amount of power needed to maintain a constant temperature between a reference cell, containing the solvent and buffer, and a sample cell, containing the ELP solution. The resulting thermogram displays a peak or valley, which indicates a change in the

state of the sample species. DSC provides an onset temperature, a temperature where the heat capacity is at its maximum, and the total change in enthalpy for the process (Figure 2.4).

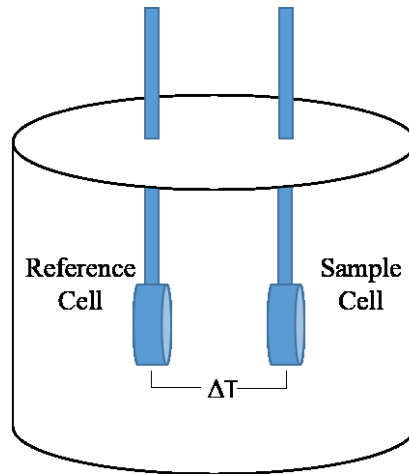


Figure 2.3 Schematic of a differential scanning calorimeter, including the reference cell (containing the solvent) and the sample cell.

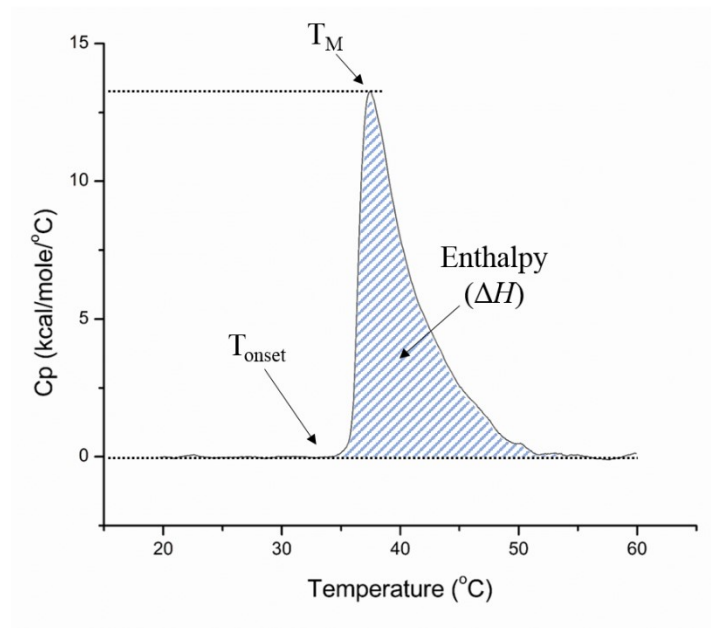


Figure 2.4 DSC curve of a 100 μM unlabeled ELP sample, scanned at a rate of 1 $^{\circ}\text{C}/\text{min}$ in PBS buffer.

REFERENCES

1. Castoldi, M.; Popov, A. V. "Purification of brain tubulin through two cycles of polymerization-depolymerization in a high-molarity buffer." *Protein Expres. Purif.* 2003, **32**, 83-88.
2. Shelanski, M. L.; Gaskin, F.; Cantor, C. R. "Microtubule Assembly in the Absence of Added Nucleotides." *Proc. Nat. Acad. Sci. USA.* 1973, **70** (3), 765-768.
3. Berkowitz, S. A.; Velicelebi, G.; Sutherland, J. W. H.; Sturtevant, J. M. "Observation of an exothermic process associated with the *in vitro* polymerization of brain tubulin." *Proc. Natl. Acad. Sci. USA.* 1980, **77** (8), 4425-4429.
4. Briguglio, I.; Laurini, E.; Pirisi, M. A.; Piras, S.; Corona, P.; Fermeglia, M.; Pricl, S.; Carta, A. "Trizolopyridinyl-acrylonitrile derivatives as antimicrotubule agents: Synthesis, *in vitro* and *in silico* characterization of antiproliferative activity, inhibition of tubulin polymerization and binding thermodynamics." *Eur. J. Med. Chem.* 2017, **141**, 460-472.
5. Banerjee, M.; Poddar A.; Mitra, G.; Surolia, A.; Owa, T.; Bhattacharyya, B. "Sulfonamide Drugs Binding to the Colchicine Site of Tubulin: Thermodynamic Analysis of the Drug-Tubulin Interactions by Isothermal Titration Calorimetry." *J. Med. Chem.* 2005 **48**, 547-555.
6. Díaz, J. F.; Buey, R. M. "Characterizing Ligand-Microtubule Binding by Competition Methods." *Method Mol. Med.* 2007, **137**, 245-260
7. Daly, E. M.; Taylor, R. E. "Entropy and Enthalpy in the Activity of Tubulin-Based Antimitotic Agents." *Curr. Chem. Biol.* 2009, **3**, 47-59.
8. Freyer, M. W.; Lewis, E. A. "Isothermal Titration Calorimetry: Experimental Design, Data Analysis, and Probing Macromolecule/Ligand Binding and Kinetic Interactions." *Methods Cell Biol.* 2008, **84**, 79–113. doi:10.1016/S0091-679X(07)84004-0

CHAPTER III

PURIFICATION OF TUBULIN USING HIGH-MOLARITY BUFFERS

Purification of tubulin can be performed in less than 14 hours using high molarity buffers to force microtubule associated proteins (MAPs) away from tubulin during polymerization and depolymerization. The most well-known method of tubulin purification from mammalian brain tissue is the Shelanski method. [1] This method involves the use of a phosphocellulose column and can take more than three days to complete. These columns are not currently commercially available. Additionally, the extended time required for running the protein solution through the column media will reduce the amount of active protein in the final solution. Purified tubulin with a high degree of activity can be purchased both with and without MAPs, but at a price that is not always cost efficient when compared to purifying the tubulin using a phosphocellulose column or high-molarity buffers. This research group used a modified purification process published by Mirco Castoldi and Andrei V. Popov at the European Molecular Biology Laboratory in Heidelberg, Germany, referred to as the Popov protocol. [2] This method uses a series of hot and cold ultracentrifugations in high molarity buffers to purify and crowd out MAPs. This process can be completed in less than 14 consecutive hours, significantly improving the activity of the final protein solution. There are five centrifugation steps in the Popov protocol which, with the exception of the first, are preceded by a cold or hot water bath to ensure complete polymerization or depolymerization of the tubulin.

The brain tissue was generously provided by Sansing Meat Processing (1815 County Line Rd, Maben, MS). Brain tissue was collected from animals, harvested, where the tissue was kept refrigerated and brought to university research lab within 6 hours of death in a cold PBS buffer (20 mM sodium phosphate, 150 mM NaCl, pH 7.2). The membrane around the brains and the blood clots were removed. The cleaned brain tissue was weighed and homogenized in a pre-cooled Warring blender with enough depolymerization buffer to cover the surface of the tissue in the blender. The tissue was blended for approximately 2 minutes in 30 second intervals. The depolymerization buffer was comprised of 50 mM of MES (2-[N-morpholino]ethane sulfonic acid) with 1 mM CaCl₂ and titrated to a final pH of 6.6 with HCl.

First ultracentrifugation: The homogenized solution was spun in 70 mL tubes in a Beckman Coulter ultracentrifuge using a pre-cooled Ti 45 rotor at 4°C at 19,300 rpm for one hour. The supernatant was collected and volume measured. Equal volumes of high-molarity 1,4-piperazinediethanesulfonic acid (PIPES) buffer and glycerol pre-heated to 37°C were added to the solution. ATP and GTP were added to the mixture to achieve final concentrations of 1.5 mM and 0.5 mM, respectively. The solution was incubated for an hour at 37°C with gentle stirring.

Second ultracentrifugation: The polymerized tubulin solution was spun at the 37°C at 44,000 rpm for forty minutes in a preheated Ti 45 rotor. The resulting pellet was collected and reconstituted in depolymerization buffer. The solution was gently stirred in a 4°C cold water bath for thirty minutes.

Third ultracentrifugation: The depolymerized tubulin solution was centrifuged at 30,000 RPM in a Ti 45 rotor at 4°C for forty minutes. The resulting supernatant from the third centrifugation was mixed with equal volumes of the high-molarity PIPES buffer and glycerol,

and ATP and GTP added for final concentrations of 1.5 mM and 0.5 mM once again. The solution was incubated at 37°C for 45 minutes in a hot water bath with gentle stirring.

Fourth ultracentrifugation: After the second hot water bath the polymerized tubulin solution was centrifuged at 44,000 rpm in a Ti 45 rotor for thirty minutes. The pellet was then collected and reconstituted with approximately 20 mL of cold BRB80 buffer. BRB80 buffer is comprised of 80 mM PIPES and 1 mM EGTA, titrated to pH 7.5 with sodium hydroxide. The solution was gently mixed in a cold water bath for 15 minutes.

Fifth ultracentrifugation: The solution was centrifuged at 4°C in a pre-cooled Type 40 rotor at 39,600 rpm. The pellet was discarded and the supernatant was collected in 2 mL aliquots and was flash-frozen with liquid N₂ and stored at -80°C until further use. Samples of the tubulin were analyzed using SDS-Gel electrophoresis and polymerization assays to assess the purity and activity of the tubulin.

Purification of tubulin from two pig brains (approximately 120 mg) resulted more than 20 mL of purified protein solution with a concentration of approximately 0.8 g/mL. The concentration was determined using the extinction coefficient $\epsilon_{280} = 115,000 \text{ M}^{-1} \text{ cm}^{-1}$. [2] SDS Gel electrophoresis was used to determine the purity of the protein solution. The resulting gel image in Figure 3.1 shows that the final solution of purified tubulin from two different trials of the original Popov protocol both contained a single band of between 48 and 63 kDa. This is in agreement with both the gel produced by Castoldi et al. using the Popov protocol and purchased tubulin from Cytoskeleton, Inc. The “PC” lane represents the Castoldi purified tubulin which has been purified using the unmodified Popov protocol. The purchased tubulin shows the purified tubulin from a modified Shelanski purification. [1] All three gels with the final tubulin solution showed that the protein did not contain any visible bands apart from the major band attributed to

the pure tubulin. The turbidity assay of the purified tubulin using the Popov protocol (Figure 3.2) shows that the protein did not polymerize within twenty minutes, but instead aggregated over three hours. Tubulin purified using a modified Shelanski method was purchased from Cytoskeleton, Inc. to compare against tubulin purified using the Popov method. Polymerization assays were used to compare their activity. All polymerization assays were performed using a Thermo Scientific NanoDrop 2000c Spectrophotometer at 37°C. The optical density was recorded at 340 nm for all assays. The assays of purchased tubulin had a short lag period and then rapidly increasing in absorption before stabilizing at the maximum degree of polymerization (Figure 3.3). The Popov protocol was reviewed and GDP was added to the cold water bath and ultracentrifugation steps to better stabilize the tubulin heterodimers (SDS-PAGE shown in Figure 3.4). This improved the purification process so that the polymerization assay followed the expected polymerization rate (Figure 3.5).

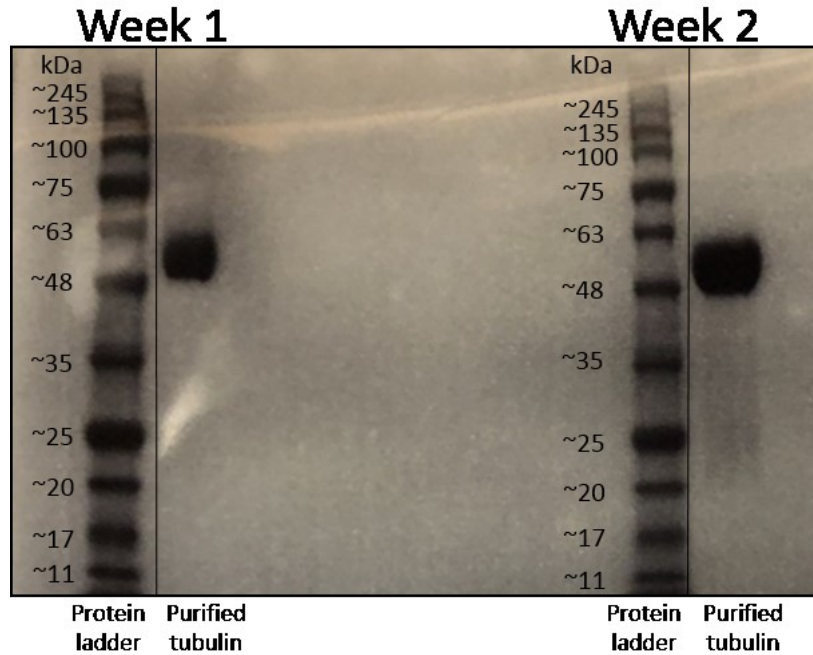


Figure 3.1 SDS-PAGE of lab purified protein using the Popov protocol. Gel stained with Coomassie blue. (A) Week 1 and (B) Week 2 of lab purified tubulin using the modified Popov protocol.

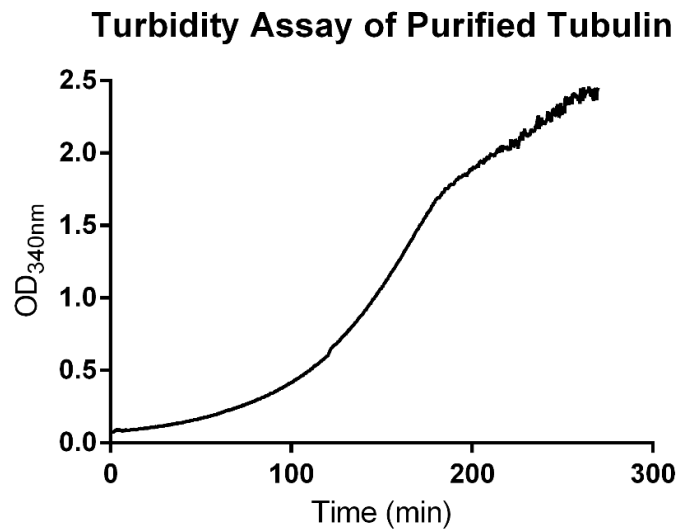


Figure 3.2 Turbidity assay of tubulin purified using the Popov method. The tubulin was selected from tubulin purified without the addition of GDP in the cold centrifugations.

Purchased Tubulin Turbidity Assay (2 mg/mL)

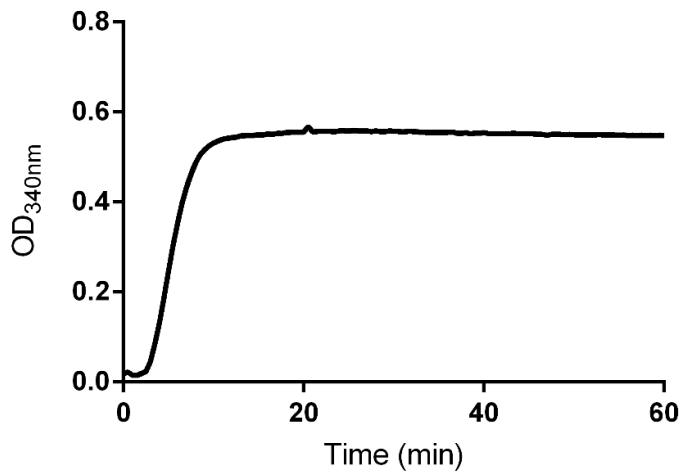


Figure 3.3 Turbidity assay of tubulin purchased from Cytoskeleton, Inc. and purified using the Shelanski method. Tubulin concentration is 2 mg/mL.

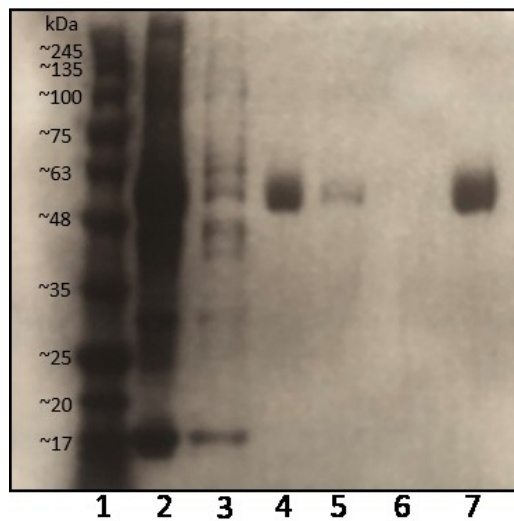


Figure 3.4 SDS Gel electrophoresis of tubulin purification using GDP. (Left to right) 1. GoldBio Bluestain protein ladder. 2. First centrifugation supernatant. 3. Second centrifugation supernatant. 4. Second centrifugation depolymerized pellet solution. 5. Third centrifugation supernatant. 6. Fourth centrifugation supernatant. (No band visible.) 7. Fifth centrifugation supernatant (final protein solution).

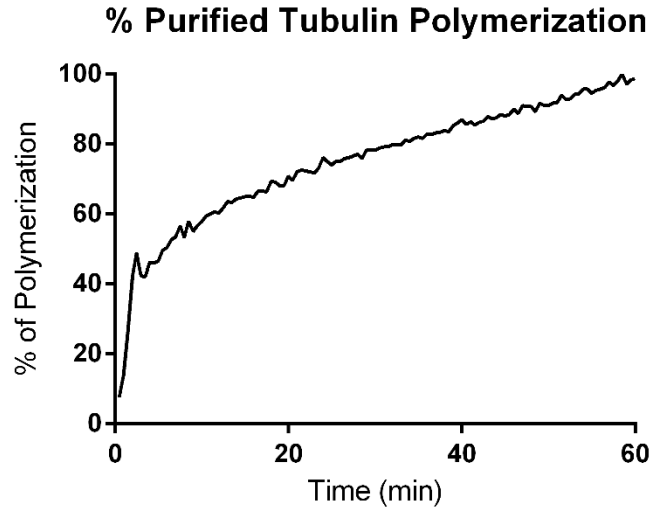


Figure 3.5 Turbidity assay of tubulin purified using improved Popov method with GDP in the cold water baths and centrifugation steps. The tubulin selected from tubulin purified without the addition of GDP in the cold centrifugations. Note that the lack of lag period can be attributed to the temperature of the tubulin being above ice water temperature.

The Popov protocol is a viable method of tubulin purification that can be used in place of the Shelanski method. It can produce approximately 15 mg of purified tubulin from 125 mg of porcine brain tissue. The original method provided by Castoldi and Popov did not include the use of guanosine 5'-diphosphate in their cold ultracentrifugation steps, though high concentrations of ATP and GTP were listed to improve polymerization in the hot water baths. The addition of GDP to the Popov protocol provided stabilization for depolymerized tubulin in the cold steps 1, 3, and 5 and greatly improved the activity of the tubulin. This modified protein purification method does not require the use of a phosphocellulose column in high-pressure liquid chromatography and produces a significant amount of tubulin in as little as 14 hours.

REFERENCES

1. Shelanski, M. L.; Gaskin, F.; Cantor, C. R. "Microtubule Assembly in the Absence of Added Nucleotides." *Proc. Nat. Acad. Sci. USA*, 1973, **70** (3), 765-768.
2. Castoldi, M.; Popov, A. V. "Purification of brain tubulin through two cycles of polymerization-depolymerization in a high-molarity buffer." *Protein Expres. Purif.* 2003, **32**, 83-88.

CHAPTER IV

EFFECT OF BINDING AGENTS AND DMSO ON THE POLYMERIZATION OF TUBULIN

Microtubules have a characteristic dynamic instability which allows the protein structure to readily lengthen or shorten as needed under different cellular conditions. [1, 2] To investigate the effect different ligands had on the polymerization of tubulin, it was necessary to be able to control tubulin polymerization.

UV-vis spectroscopy was used to turbidimetrically monitor the polymerization of tubulin into microtubules. The absorbance was recorded at 340 nm, which is considered proportional to the degree of polymerization. The polymerization assays were performed using a 1 cm pathlength and 5 mm wide cuvette that was pre-cooled on ice. Tubulin purchased from Cytoskeleton, Inc. (cat. #T240) was reconstituted in a pre-cooled polymerization buffer. The Thermo Scientific NanoDrop 2000c Spectrophotometer was preheated to 37°C and the assay performed with 2 mg/mL tubulin. The absorbance was recorded every thirty seconds for a minimum of one hour or until the absorbance has approximately stopped increasing or could not be recorded at any higher absorbance. Ligands were added to the polymerization buffer at a nominal concentration of 10 µM before reconstitution. The extinction coefficient used for determining the concentration of RPC2 was $\epsilon_{460} = 30,000 \text{ M}^{-1} \text{ cm}^{-1}$ and was provided by Dr. Fred Macdonnell with the ligand samples. The extinction coefficient used for determining the concentration of docetaxel and colchicine are $\epsilon_{274} = 1,730 \text{ M}^{-1} \text{ cm}^{-1}$ and $\epsilon_{350} = 16,600 \text{ M}^{-1} \text{ cm}^{-1}$, respectively. [3, 4]

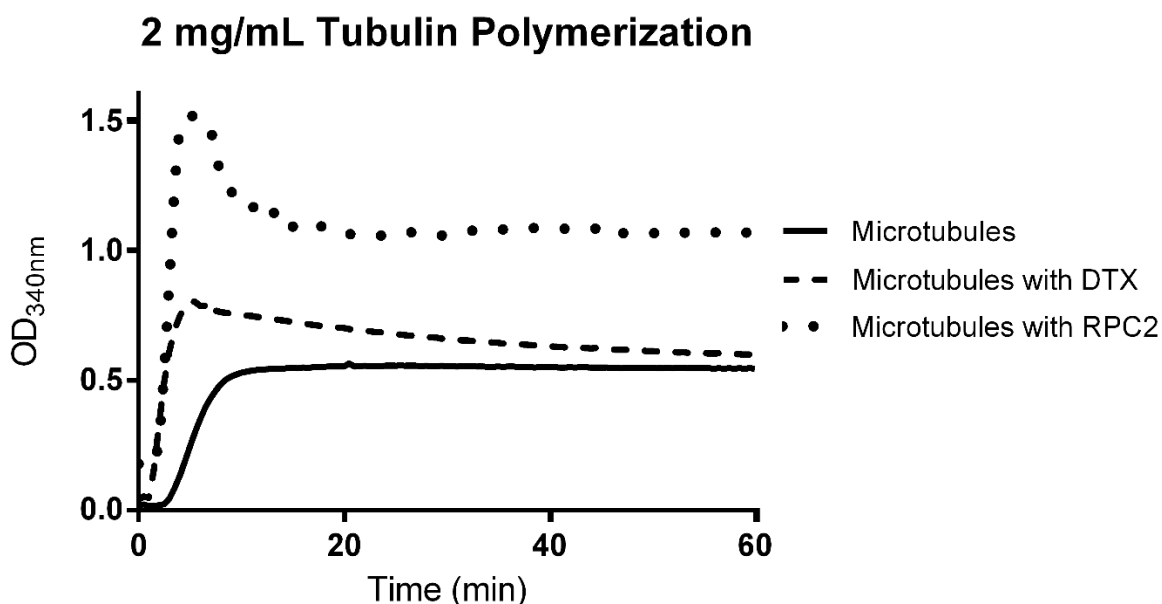


Figure 4.1 Polymerization assays of 2 mg/mL tubulin at 37°C. All concentrations were 2 mg/mL and ligand concentrations were 10 μ M.

The polymerization assays shown in Figure 4.1 display how tubulin of sufficient concentration polymerizes through GTP hydrolysis linking α/β -monomers together in protofilaments, which twist together in a cylindrical structure. [5] The RPC2 and docetaxel ligands were stored in DMSO due to low solubility in aqueous solution. Therefore, the polymerization assays containing approximately 10 μ M RPC2 or docetaxel contain 3% DMSO. The addition of both RPC2 and docetaxel shortened the initial lag period expected in tubulin polymerization assays before rapidly increasing in absorbance. The addition of docetaxel did not significantly increase the concentration of microtubules at the final polymerization rate, but the addition of RPC2 caused the final OD₃₄₀ of the assay to almost double. The increase in light scattering can be attributed to either an increase in the amount of microtubules that have formed at the final polymerization rate or to the possibility that docetaxel and RPC2 alter the

microtubule structure when initially binding to the tubulin α/β -heterodimers and increase turbidity. In contrast, colchicine is verified to be a destabilizing agent. Polymerization does not appear to occur at all, and instead is aggregating. The lag period is severely extended and the absorbance does not level off, but rather continues increasing over an extended 11 period of time until the absorbance could no longer be accurately read in this instrument (Figure 4.2). Docetaxel is a known microtubule stabilizer and colchicine a known destabilizing agent. Comparison of the assays performed have shown that tubulin polymerized with RPC2 behaves more similarly to tubulin bound with stabilizing agents than destabilizing agents.

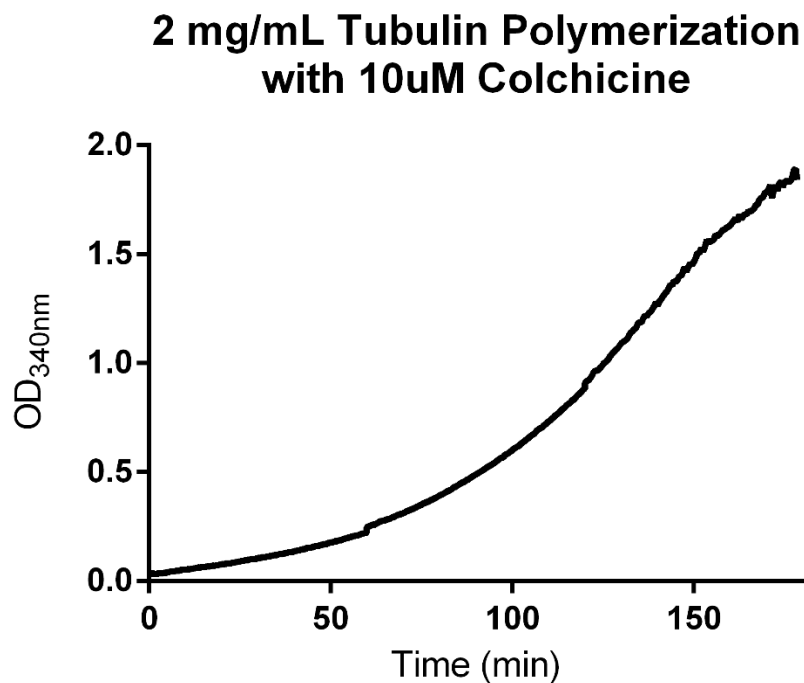


Figure 4.2 Polymerization assays of 2 mg/mL tubulin with 10 μ M at 37°C. Tubulin was purchased from Cytoskeleton, Inc. and purified using the Shelanski method.

Polymerization assays performed with the addition of DMSO and no ligand showed a sharp increase in absorbance before leveling to the final absorbance, which could be attributed to

the formation of a sheet of protofilaments before folding into the complete cylindrical microtubule. [6, 7, 8] The sharp increase in absorbance of the ligand-bound polymerization assays is shown to be attributed to the addition of DMSO, but the final absorbance was not significantly affected by the solution containing 3% DMSO. Polymerization assays comparing tubulin polymerized with 3% DMSO (v/v) and without (Figure 4.3). [8]

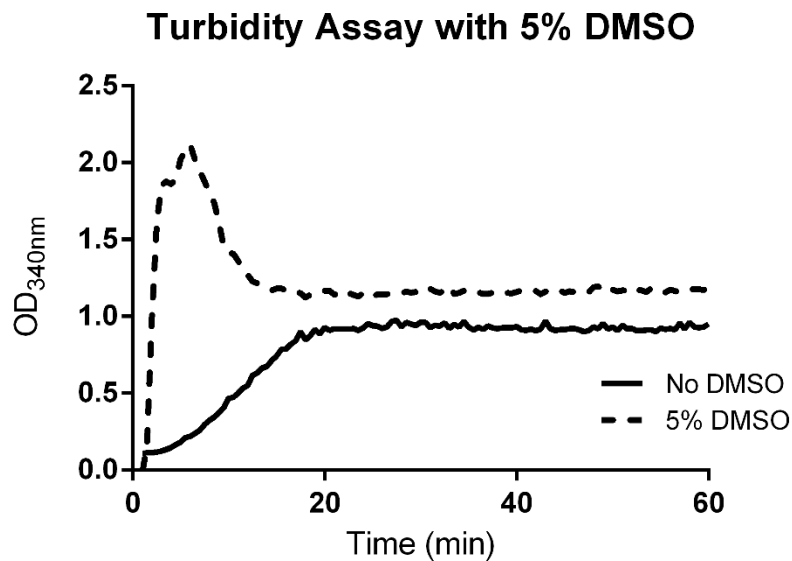


Figure 4.3 Polymerization assay of 2 mg/mL tubulin with and without 5% DMSO. The tubulin sample was purchased from Cytoskeleton, Inc. and purified using the Shelanski method. [7]

REFERENCES

1. Wade, R. W. "On and Around Microtubules: An Overview." *Mol. Biotechnol.* 2009, **43**, 177-191
2. Howard, J.; Hyman, A. A. "Dynamics and mechanics of the microtubule plus end." *Nature*, 2003, **422**, 753-758.
3. O'Neil, M. J. (ed.) "The Merck Index – An Encyclopedia of Chemicals, Drugs, and Biologicals." Royal Society of Chemistry: Cambridge, UK 2013. p. 620.
4. Mons, S.; Veretout, F.; Carlier, M.; Erk, I.; Lepault, J.; Trudel, E.; Salesse, C.; Ducray, P.; Mioskowski, C.; Lebeau, L. "The interaction between lipid derivatives of colchicine and tubulin: Consequences of the interaction of alkaloid with lipid membranes." *Biochim. Biophys. Acta*, 2000, **1468** (1-2), 381-395.
5. Mari, C.; Pierroz, V.; Ferrari, S.; Gasser, G. "Combination of Ru(II) complexes and light: new frontiers in cancer therapy." *Chem. Sci.* 2015, **6**, 2660-2686.
6. Banerjee, M.; Poddar, A.; Mitra, G.; Surolia, A.; Owa, T.; Bhattacharyya, B. "Sulfonamide Drugs Binding to the Colchicine Site of Tubulin: Thermodynamic Analysis of the Drug-Tubulin Interactions by Isothermal Titration Calorimetry." *J. Med. Chem.* 2005 **48**, 547-555.
7. Díaz, J. F.; Buey, R. M. "Characterizing Ligand-Microtubule Binding by Competition Methods." *Method Mol. Med.* 2007, **137**, 245-260
8. Daly, E. M.; Taylor, R. E. "Entropy and Enthalpy in the Activity of Tubulin-Based Antimitotic Agents." *Curr. Chem. Biol.* 2009, **3**, 47-59.
9. Algaier, J.; Himes, R. H. "The effects of dimethyl sulfoxide on the kinetics of tubulin assembly." *Biochim. Biophys. Acta*, 1988, **954**, 235-243.

CHAPTER V

BIOPHYSICAL BINDING PROPERTIES OF $[\text{Ru}(\text{Ph}_2\text{Phen})_3]^{2+}$ TO MICROTUBULES

The binding of ligands such as colchicine and docetaxel to microtubules has been investigated for a few decades, but the thermodynamic properties of their binding had not been successfully determined and compared to known microtubule-binding agents. [1] This study used isothermal titration calorimetry to determine the enthalpy, entropy and free energy of these ligands so that they could be compared to thermodynamic values for $[\text{Ru}(\text{Ph}_2\text{phen})_3]^{2+}$ binding to tubulin. Docetaxel and colchicine both have known and distinct binding locations on microtubules. Docetaxel is a tubulin-stabilizing agent that binds to the taxane site on the β -subunit of tubulin heterodimers and inhibits depolymerization of tubulin, inducing apoptosis. [2, 3, 4] Colchicine is a destabilizing binding agent, which binds between the α and β subunits and causes rapid depolymerization, inducing apoptosis. [5] If these binding agents caused a significant change in the polymerization or depolymerization rate mid-experiment, then the results would be very difficult to interpret. This study manipulated the tubulin samples as described below so that they were not capable of forming microtubules or could not polymerize to a higher degree under experimental conditions. The control of the polymerization rate of tubulin was controlled through careful temperature control.

Unpublished experiments by Dr. Frederick Macdonnell's research group have shown that paclitaxel (an analog of docetaxel) binds to microtubules and can alter its structure by transmission electron microscopy (Figure 5.1). The microtubules increase in thickness and

appear more rigid, with more easily definable borders. Transmission electron microscopy with RPC2 bound microtubules showed microtubules that appear similar in length and thickness,. Electron microscopy with destabilizing agents such as colchicine were not performed.

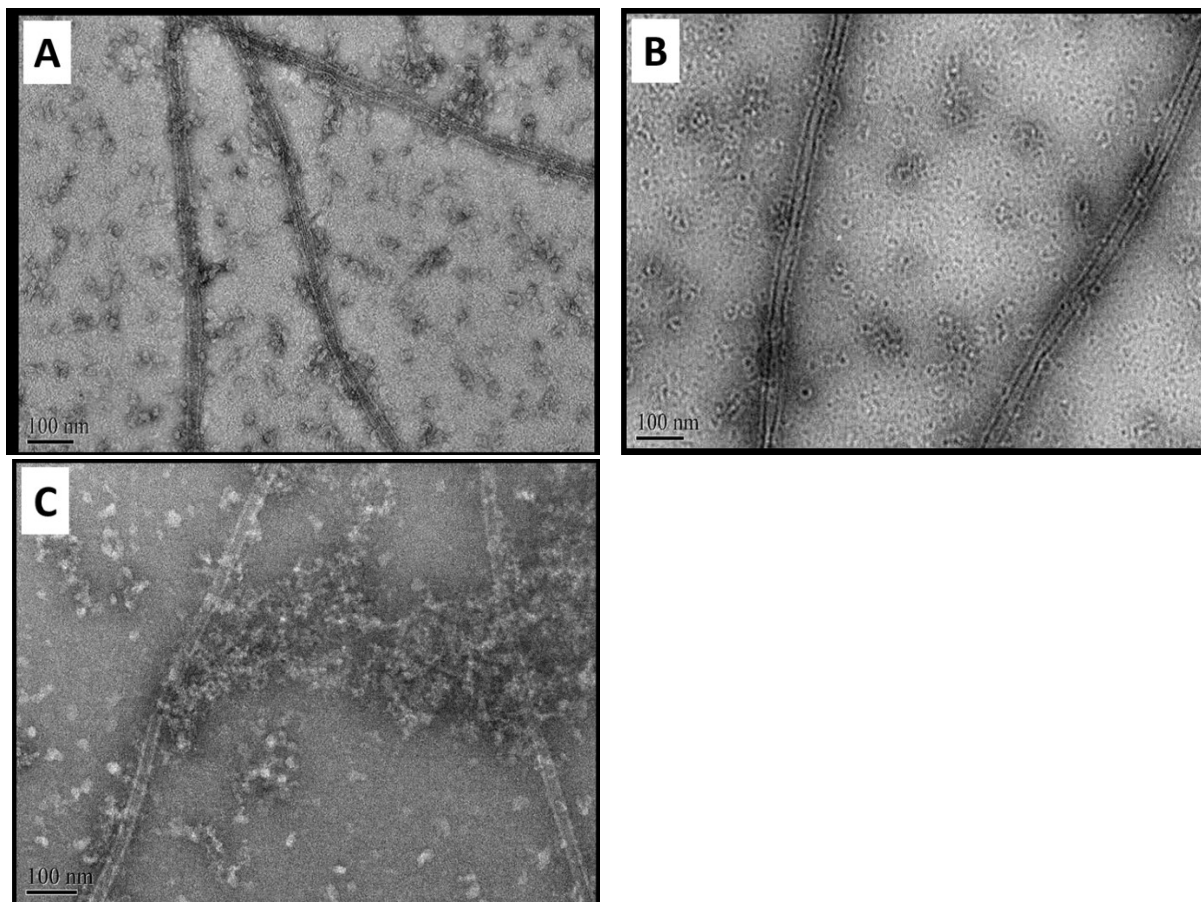


Figure 5.1 Transmission electron micrographs (provided by Dr. Frederick Macdonnell) of (A) tubulin polymerized in the absence of any ligands, (B) tubulin polymerized with 10 μM paclitaxel, (C) tubulin polymerized with 10 μM RPC2. The samples were stained with 1% (w/v) uranyl acetate on 300-mesh carbon-coated, formvar-treated copper grids. The grids were studied in a Zeiss model 10CA electron microscope and the bar scale is 100 nm.

Reverse titrations were used in all ITC experiments due to the extremely low solubility of RPC2 in aqueous solutions. Typical ITC experiments involved fourteen 20 μL injections of tubulin ($\sim 30 \mu\text{M}$ heterodimers, or 2 mg/mL) into a 1.45 mL cell of ligand solution. The ligand

concentrations were determined using UV-vis spectroscopy and varied due to varying solubility in the buffer solutions. The extinction coefficient used for determining the concentration of RPC2 was $\epsilon_{460} = 30,000 \text{ M}^{-1} \text{ cm}^{-1}$ and was provided by Dr. Fred Macdonnell with the ligand samples. The extinction coefficient used for determining the concentration of docetaxel and colchicine are $\epsilon_{274} = 1,730 \text{ M}^{-1} \text{ cm}^{-1}$ and $\epsilon_{350} = 16,600 \text{ M}^{-1} \text{ cm}^{-1}$, respectively. [6, 7] Tubulin concentration was kept below 3 mg/mL to ensure that minimal microtubule formation before any polymerization assays were performed in preparation for ITC experiments. A MicroCal VP-ITC (Malvern) instrument was used at 37°C, when using polymerized tubulin, and 4°C, when using depolymerized tubulin. CHASM, an ITC data analysis program developed in the Lewis Biophysics Laboratory, was used to fit the ITC titrations and to determine the thermodynamic parameters, including the association constant (K) and changes in free energy (ΔG), enthalpy (ΔH), and entropy ($-T\Delta S$). [8]

Figure 5.2 shows the integrated ITC data for the titration of docetaxel with depolymerized tubulin and microtubules. The stoichiometry suggests a binding of 1:1 docetaxel:tubulin heterodimer at saturation for both experiments. [2, 3, 4] The ITC experiments binding depolymerized tubulin to RPC2 or colchicine are not shown below. Injecting depolymerized tubulin into RPC2 created excessive heat, consistent with an increase in the microtubule polymerization rate, and produced a thermogram that could not be fitted due to the large amount of noise in the raw data. ITC experiments injecting depolymerized tubulin into colchicine produced insufficient heat to successfully determine the binding parameters. RPC2 binding to polymerized tubulin is shown below in Figure 5.3 and has a binding ratio of approximately 1:1. Colchicine binds to polymerized tubulin heterodimers in approximately a 1:1 ratio. This is similar to what we see in the competitive experiment below in Figure 5.4 where

colchicine is bound to microtubules that have been polymerized with RPC2 in the solution. The enthalpy of these experiments greatly differs, suggesting a different binding mode of colchicine with RPC2 polymerized microtubules.

Competitive ITC experiments show binding in a 1:1 ratio of RPC2 to microtubules polymerized with docetaxel. The binding affinity of RPC2 appears lower than experiments binding RPC2 to ligand-free microtubules. Microtubules polymerized with RPC2 and injected into colchicine showed a higher binding affinity than when bound to ligand-free microtubules and had a 1:1 binding ratio. The nonlinear regression fits of experiments binding docetaxel to tubulin polymerized with RPC2 could not be produced as they did not release sufficient heat to successfully determine the binding parameters. The best fit parameters, (K , ΔH , n), and the Gibbs free energy (ΔG), and the change in entropy term ($-T\Delta S$) for each titration are shown below in the table below.

Table 5.1 ITC-derived thermodynamic parameters for the binding of docetaxel, colchicine, and RPC2 in non-competitive and competitive experiments

Complex	Ligand	K (M ⁻¹)	ΔG (kcal mol ⁻¹)	ΔH (kcal mol ⁻¹)	$-T\Delta S$ (kcal mol ⁻¹)
Tubulin	Docetaxel	$8.1 \cdot 10^6$	-9.4 ± 1.0	-28.7 ± 4.1	19.2
MT	Docetaxel	$5.5 \cdot 10^6$	-9.2 ± 0.9	-33.4 ± 6.5	24.7
MT	RPC2	$4.9 \cdot 10^6$	-9.1 ± 0.9	-16.7 ± 2.3	7.6
MT	Colchicine	$5.0 \cdot 10^6$	-9.1 ± 0.9	-12.8 ± 2.4	3.7
MT:DTX	RPC2	$2.0 \cdot 10^6$	-8.6 ± 0.9	-14.6 ± 7.7	6.0
MT:RPC2	Colchicine	$7.6 \cdot 10^6$	-9.4 ± 0.9	-33.9 ± 7.3	24.5

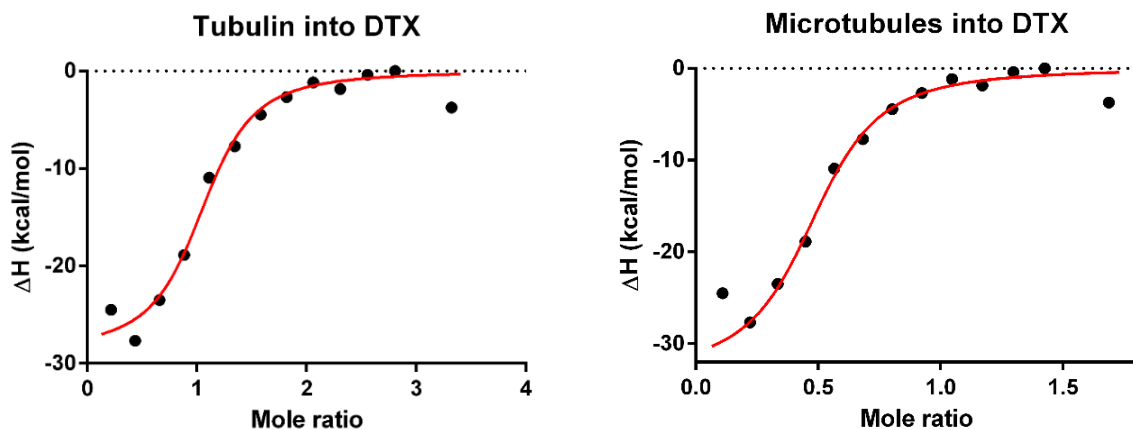


Figure 5.2 Nonlinear regression fits of the ITC integrated heat data for docetaxel binding to depolymerized tubulin and microtubules.

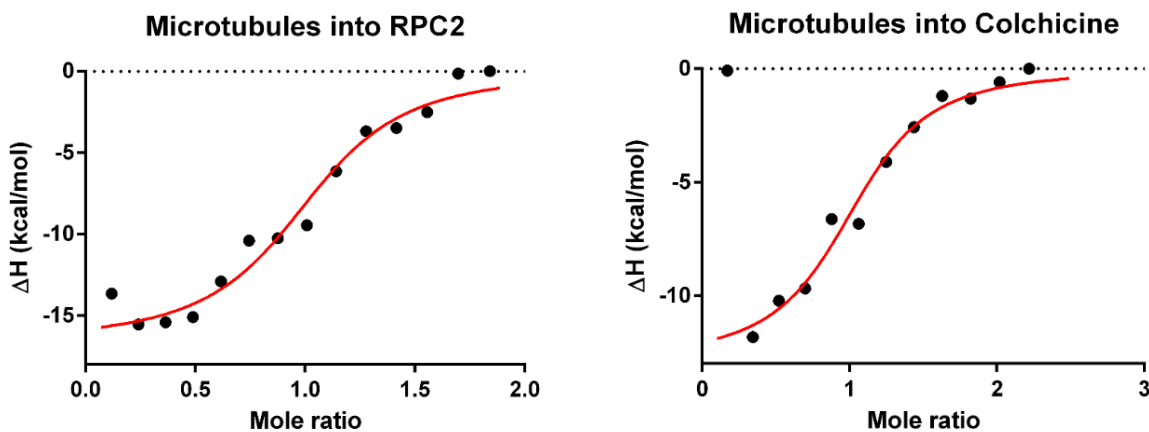


Figure 5.3 Nonlinear regression fit of the ITC integrated heat data for RPC2 and colchicine binding to microtubules.

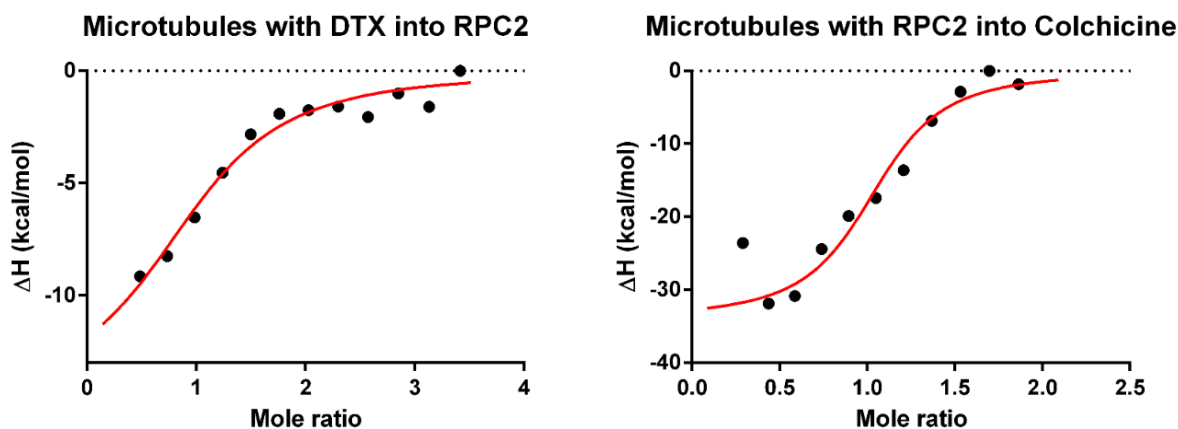
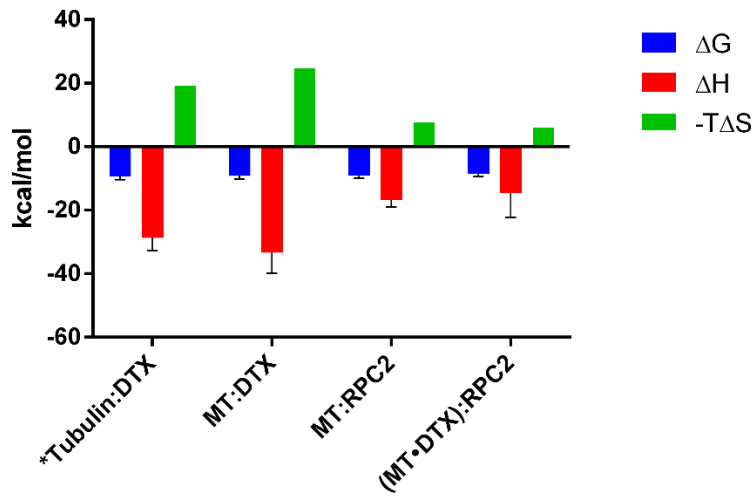


Figure 5.4 Nonlinear regression fits of the ITC integrated heat data for competitive experiments.

Figure 5.5 compares the Gibbs free energy, enthalpy, and change in entropy of the experiments. The Gibbs free energy of all of these experiments were very similar, with varying entropy and enthalpy that increase in tandem and appear to compensate for one another. The thermogram for depolymerized tubulin binding to RPC2 is not shown as the heat produced from these injections produced irregular thermograms that could not be fitted. This is attributed to RPC2 binding to trace amounts of tubulin heterodimers and causing polymerization of the injected tubulin, even at 4°C. The ΔH of RPC2 binding to ligand-free microtubules and docetaxel-bound microtubules is roughly equal to the difference of docetaxel binding to microtubules and RPC2 binding to microtubules, indicating that the polymerized tubulin shows preferential binding to RPC2 in this experiment. Experiments injecting microtubules formed with RPC2 into docetaxel produced insufficient heat to determine the binding parameters, suggesting that the altered structure of microtubules polymerized with RPC2 may have an alter taxane binding site that does not support docetaxel binding (Figure 5.1 C).

ITC experiments injecting depolymerized tubulin into colchicine showed little to no binding and did not induce polymerization, which was expected from this microtubule destabilizing agent. Injecting polymerized microtubules into colchicine showed binding without extensive induced depolymerization under experiment conditions. The ΔH and $-T\Delta S$ are larger for colchicine binding with microtubules formed with RPC2 (Figure 5.5). Despite this binding, the microtubules do not appear to undergo induced depolymerization. This indicates that colchicine and RPC2 do not compete for binding locations on the of microtubule:RPC2 complex. This is supported by the binding ratio for colchicine almost doubling when binding to RPC2-polymerized microtubules. The difference in thickness and length may provide more space for colchicine to bind to the tubulin.



*The 1st reagent is the titrant and the 2nd reagent is in the calorimeter cell.

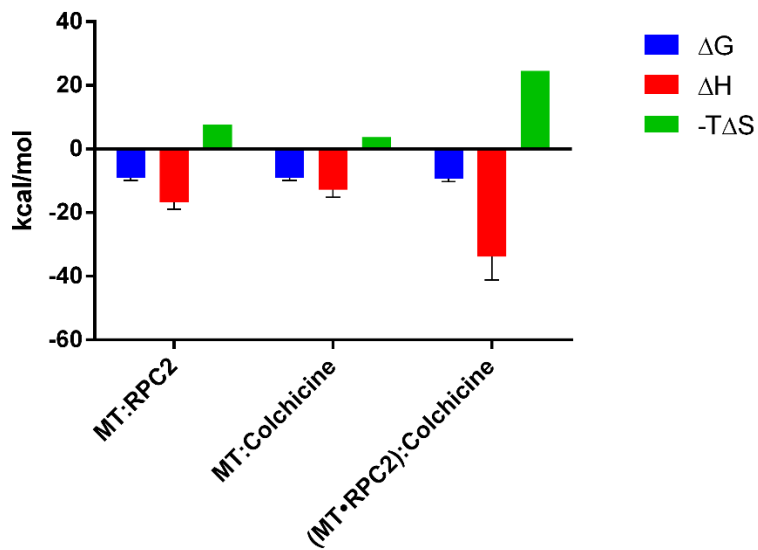


Figure 5.5 Thermodynamic profiles for ligand binding to polymerized and depolymerized tubulin.

REFERENCES

1. Mari, C.; Pierroz, V.; Ferrari, S.; Gasser, G. "Combination of Ru(II) complexes and light: new frontiers in cancer therapy." *Chem. Sci.* 2015, **6**, 2660-2686.
2. Schilstra, M. J.; Bayley, P. M.; Martin, S. R. "The effect of solution composition on microtubule dynamic instability." *Biochem. J.* 1991, **277**, 839-947.
3. Magnani, M.; Maccari, G.; Andreu, J. M.; Diaz, J. F.; Botta, M. "Possible binding site for paclitaxel at microtubule pores." *FEBS J.* 2009, **276**, 2701-2712.
4. Tommasi, S.; Mangia, A. Lacalamita, R. Bellizzi, A. Fedele, V. Chiriatti, A; Thomssen, C. Kendzierski, N.; Latorre, A.; Lorusso, V.; Schittulli, F.; Zito, F.; Kavallaris, M. Paradiso, A. "Cytoskeleton and paclitaxel sensitivity in breast cancer: The role of β -tubulins." *Int. J. Cancer*, 2007, **120** 2078-2085.
5. Buey, R. M.; Díaz, J. F.; Andreu, J. M.; O'Brate, A.; Giannakakou, P.; Nicolaou, K. C.; Sasmal, P. K.; Ritzén, A.; Namoto, K. "Interaction of Epothilone Analogs with the Paclitaxel Binding Site: Relationship between Binding Affinity, Microtubule Stabilization, and Cytotoxicity." *Chem. Biol.* 2004, **11**, 225-236.
6. O'Neil, M. J. (ed.) "The Merck Index – An Encyclopedia of Chemicals, Drugs, and Biologicals." Royal Society of Chemistry: Cambridge, UK 2013. p. 620.
7. Mons, S.; Veretout, F.; Carlier, M.; Erk, I.; Lepault, J.; Trudel, E.; Salesse, C.; Ducray, P.; Mioskowski, C.; Lebeau, L. "The interaction between lipid derivatives of colchicine and tubulin: Consequences of the interaction of alkaloid with lipid membranes." *Biochim. Biophys. Acta*, 2000, **1468** (1-2), 381-395.
8. Freyer, M. W.; Lewis, E. A. "Isothermal Titration Calorimetry: Experimental Design, Data Analysis, and Probing Macromolecule/Ligand Binding and Kinetic Interactions." *Methods Cell Biol.* 2008, **84**, 79–113. doi:10.1016/S0091-679X(07)84004-0

CHAPTER VI
THERMAL STABILITY OF SYN-B1 ELASTIN-LIKE POLYPEPTIDE AND
DOXORUBICIN

The thermodynamic behavior of the elastin-like polypeptide (ELP) sequence SynB1-Cys-ELP1, derived from tropoelastin, was investigated using differential scanning calorimetry. This ELP consists of a 150 pentapeptide repeat of $[VPG(V_5G_3A_2)G]_{150}$ with a cysteine engineered into the sequence for covalent drug attachment and a SynB1 cell-penetrating peptide at the N-terminus. The SynB1 cell-penetrating peptide is designed to increase ELP uptake by cells, especially tumor cells via endocytosis. [1, 2] This ELP was investigated to determine its effectiveness as a drug carrier for the thermal targeted delivery of doxorubicin (Dox). DSC measurements show that the ELP undergoes a liquid-liquid phase separation beginning at the lower critical solution temperature that can be enhanced by Dox labeling. The ELP phase transition is monophasic and the transition of mixed unlabeled and Dox-label ELP is biphasic, with the Dox-labeled ELP transition beginning at a lower temperature. The difference in the change in enthalpy between unlabeled and Dox-labeled ELP is consistent with droplet formation stabilized by favorable enthalpic interactions. [2]

Differential scanning calorimetry is used to analyze thermodynamic parameters of the liquid-liquid phase transition without assumptions about the mechanism. [2, 3] Prepared ELP samples were provided by Dr. John Correia's research group at the University of Mississippi Medical Center and were kept frozen at -20°C until thawed for use in DSC experimentation. The

thermograms for unlabeled, 90% Dox-labeled, and 45% Dox-labeled ELP heated at a rate of 1°C/min are shown in Figure 21. All thermograms heated at this rate showed an asymmetrical transition that has been previously observed in ELP liquid-liquid phase transitions [1] as a result of molecular association and the ongoing phase change at higher temperatures. [1, 2, 3] This shoulder produced by the continuing phase change was significantly reduced when unlabeled and Dox-labeled ELP samples were heated at a rate of 0.2°C/min with negligible differences in enthalpy (Figure 6.1).

Table 6.1 Thermodynamic parameters of obtained from unlabeled and Dox-labeled SynB1-Cys-ELP samples

Sample	Concentration	Percent Labelled	Scan Rate	T _i (°C)	T _{Peak 1} (°C)	T _{Peak 2} (°C)	ΔH (kcal/mol)
Unlabeled Trial 1	100 μM		1 °C/min	34.8 ± 0.2		37.5 ± 0.2	72.6 ± 2.0
Unlabeled Trial 2	100 μM		1 °C/min	35.0 ± 0.2		36.5 ± 0.2	75.8 ± 2.0
Unlabeled Trial 3	90 μM		1 °C/min	35.0 ± 0.2		36.7 ± 0.2	65.2 ± 2.0
Unlabeled Trial 4	90 μM		0.2 °C/min	36.0 ± 0.2		36.9 ± 0.2	62.5 ± 2.0
DOX Labeled Trial 1	100 μM	93%	1 °C/min	29.3 ± 0.2	31.3 ± 0.2		70.8 ± 2.0
DOX Labeled Trial 2	100 μM	90%	1 °C/min	29.5 ± 0.2	31.2 ± 0.2		63.5 ± 2.0
DOX Labeled Trial 3	100 μM	46.5%	1 °C/min	29.5 ± 0.2	32.8 ± 0.2	38.0 ± 0.2	87.8 ± 2.0
DOX Labeled Trial 4	100 μM	45.0%	1 °C/min	28.1 ± 0.2	33.1 ± 0.2	38.8 ± 0.2	82.4 ± 2.0

DSC T_i, T_{Peak}, and enthalpy values for unlabeled and Dox-labeled SynB1-Cys-ELP. Experiments were run at either 90 or 100 μM at a rate of 1 °C/min, with the exception of Unlabeled ELP Trial 4, which was 0.2 °C/min. All ELP samples were in a phosphate-buffered saline (PBS) and were provided by Dr. Jack Correia from the University of Mississippi Medical Center.

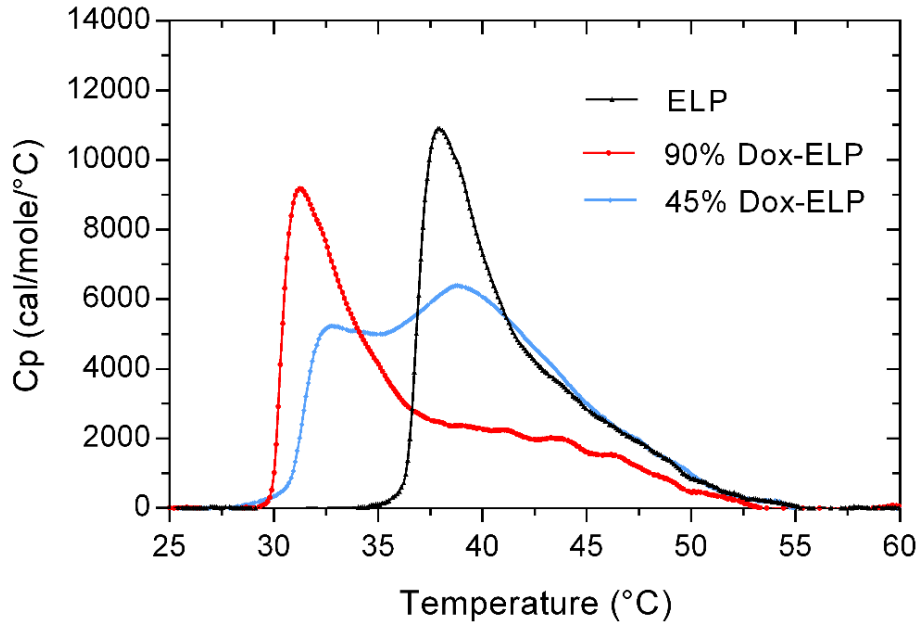


Figure 6.1 DSC curve of unlabeled SynB1-ELP, 45% Dox-labeled SynB1-ELP, and 90% Dox-labeled SynB1-ELP scanned at a rate of 1°C/min.

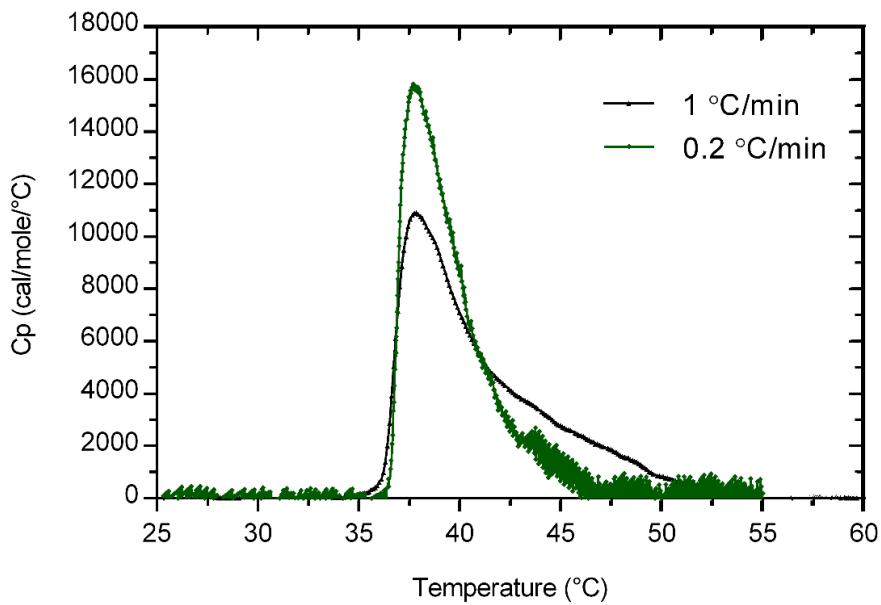


Figure 6.2 DSC curve of unlabeled SynB1-ELP scanned at a rate of 1°C/min and 0.2°C/min.

The enthalpy of the transitions was determined by integrating the excess heat capacity of the measured temperature range. The enthalpy values (Table 6.1) at 1°C/min were averaged over two runs and were 76.0 kcal/mol for unlabeled ELP, 65.7 kcal/mol for 90% Dox-labeled ELP, and 70.2 kcal/mol for 45% Dox-labeled ELP. Comparison of 1°C/min and 0.2°C/min scan rates with unlabeled ELP showed a negligible difference between the resulting enthalpies. The 45% Dox-labeled ELP was biphasic, consistent with the observations by Dreher *et al.* [4] The enthalpic enhancement of the phase transition between unlabeled and 90% Dox-labeled ELP extrapolated to 100% suggests that Dox-labeling has a -11.4 kcal/mol stabilizing effect on the coacervate. The thermograms demonstrate a broad 5-6°C phase change above the initial T_i region. The positive ΔH of the liquid-liquid phase transition is consistent with the burial of the hydrophobic surface and the favorable change in enthalpy from Dox-labeling consistent with direct Dox-ELP interactions in the coacervates. [2] These experiments show that the addition of the Dox label significantly lowers the enthalpy of the transition and has a stabilizing effect on the coacervate, plausibly through van der Waals interactions. [2, 5]

REFERENCES

1. Weisenberg, R. C.; Borisy, G. G.; Taylor, E. W. "The Colchicine-Binding Protein of Mammalian Brain and Its Relation to Microtubules." *Biochemistry*, 1968, **7** (12), 4466-4479.
2. Lyons, D. F.; Le, V.; Kramer, w. H.; Bidwell, G. L.; Lewis, E. A.; Raucher, D.; Correia, J. J. "Effect of basic cell-penetrating peptides on the structural, thermodynamic, and hydrodynamic properties of a novel drug delivery vector, ELP[V5G3A2-150]." *Biochemistry*, 2014, **53** (6), 1081-1091.
3. Zai-Rose, V.; West, S. J.; Kramer, W. H.; Bishop, G. R. Lewis, E. A.; Correia, J. J. "Effects of Doxorubicin on the Liquid-Liquid Phase Change Properties of Elastin-Like Polypeptides." *Biophys.l J.* 2018, **115**, 1-14.
4. Sturtevant, J. M. "Biochemical Applications of Differential Scanning Calorimetry." *Annu. Rev. Phys. Chem.* 1987, **38**, 463-488.
5. Dreher, M. R.; Raucher, D.; Chilkoti, A. "Evaluation of an elastin-like polypeptide-doxorubicin conjugate for cancer therapy." *J. Control Release*, 2003, **91**, 31-43.